INTERNATIONAL ATOMIC ENERGY AGENCY
UNITED NATIONS EDUCATIONAL, SCIENTIFIC AND CULTURAL ORGANIZATION

INTERNATIONAL CENTRE FOR THEORETICAL PHYSICS
34100 TRIESTE (ITALY) - P.O.B. 586 - MIRAMARE - STRADA COSTIERA 11 - TELEPHONE: 2240-1
CABLE: CENTRATOM - TELEX 460392-1

H4.SMR/204 - 38

WINTER COLLEGE ON

ATOMIC AND MOLECULAR PHYSICS

(9 March - 3 April 1987)

ATMOSPHERIC DIAGNOSTICS

S. SVANBERG

Lund Institute of Technology
S-221 00 Lund
Sweden

A MOBILE REMOTE SENSING SYSTEM FOR ATMOSPHERIC MONITORING

H. Edner, K. Fredriksson*, A. Sunesson, S. Svanberg,

L. Unéus, and W. Wendt

Lund Institute of Technology, Department of Physics,

P.O. Box 118, S-221 00 Lund, Sweden

*Swedish National Environment Protection Board,

Lund Institute of Technology, P.O. Box 118, S-221 00 Lund, Sweden

Abstract

A mobile optical remote-sensing system for environmental monitoring is described. The system, housed in a full-size truck with a laboratory floor surface of 6.0 x 2.3 m^2, is mainly intended for differential absorption lidar (DIAL) applications, but can also be used for laser-induced fluorescence monitoring and for absorption measurements using classical light sources. The system has a 40-cm diameter receiving telescope and a fully steerable flat mirror in a transmitting/receiving dome. A Nd:YAG-pumped dye laser with auxiliary non-linear frequency conversion is the preferred transmitter in DIAL measurements. Measurement examples for atmospheric SO_2 and NO_2 monitoring with automatic concentration map drawings are given and further applications are discussed.

1. Introduction

Optical and laser remote-sensing techniques provide powerful tools for environmental monitoring. In particular, atmospheric pollution levels and meteorological parameters can be determined, with range resolution, by laser techniques employing lidar (light detection and ranging) and DIAL (differential absorption lidar) methods[1,2]. Long-path absorption measurements can also be performed with classical light sources using the differential optical absorption spectroscopy (DOAS) technique[3,4]. Powerful methods for pollution monitoring are obviously of considerable interest in view of health hazards, soil and lake acidification and forest damage. A mobile system with advanced electro-optical and computer equipment makes air pollution monitoring in industrial and urban areas possible. Such a system is described in the present paper and selected measurement examples illustrate the capabilities of the system and the techniques used.

Our group has been involved in atmospheric remote sensing using laser techniques for quite some time. Based on experience from early field tests[5] a compact mobile lidar system was completed in 1979[6]. This system has undergone extensive field testing, leading to a critical assessment of the capabilities and limitations in air pollution measurements using laser techniques[7-10]. While this system was very convenient for SO_2, NO_2 and particle monitoring, the rather limited laboratory space restricted developmental work on various transmitter and detection combinations. The new system described in this paper has all the versatility needed for technique development, e.g. within the lidar, DIAL, gas correlation lidar[11], fluorescence lidar[12] and DOAS

fields. It can also be very useful for different kinds of electro-optical measurements in an industrial environment (see e.g. Ref. 13). A photograph of the system with its retractable transmission/reception dome in operational position is shown in Fig. 1, which also shows a 20 kVA motor generator unit providing power in the field. When the system is at its home base it is docked to the building and constitutes another fixed laboratory with advanced electro-optical and computer equipment.

While the new system is intended for all kinds of exploratory optical remote-sensing work and has great flexibility, it is at present arranged for DIAL measurements. The system description given below focuses on this and the measurement examples given for the system in operation are DIAL measurements. The principle of DIAL has been discussed in detail, e.g. in Refs 2, 6. Rather than reviewing the mathematical framework for DIAL, we have chosen to demonstrate the operational principles in pictorial form (Fig. 2).

In part a) of this figure a typical pollution measurement situation is depicted. Two industrial stacks produce plumes containing the gaseous pollutant, e.g. SO_2. The laser beam from the DIAL system is transmitted through the gas clouds that spread through the atmosphere. The laser pulse length is typically 5-10 ns, corresponding to a range resolution of about 1 m. For simplicity, the atmosphere is assumed to contain a uniform distribution of scattering particles. In part b) the received backscattered intensity is shown as a function of distance (delay time) for the case where the laser is tuned to an absorption band of the molecule and when the laser is tuned to a neighbouring wavelength where less or no absorption occurs. For pulses of equal energy and neighbouring wavelengths the two curves will be identical

with a $1/R^2$ fall-off for distances up to the first gas cloud. The smooth curves are due to collected laser light that has been elastically backscattered by the uniform particle and molecule distribution. However, when the laser pulse propagates through the gas clouds the situation differs. The non-absorbed wavelength is unaffected by the gas and the backscattered intensity (full line) continues its $1/R^2$ fall-off. The light at the absorption wavelength is attenuated through a cloud according to Beer-Lambert's law, and the backscattered light in and behind the cloud is again attenuated on its way back to the telescope (dashed line). The intensity behind the cloud continues its $1/R^2$ fall-off but at a reduced level. Upon passage through the last, dense gas cloud a substantial fall-off occurs. The two curves illustrate the outcome of an evaluation of the general lidar equation[1,2] for the non-absorbed and the absorbed wavelengths, respectively. The difference between the curves can best be illustrated by dividing the latter curve by the former one for every distance (delay time). The result is shown in part c) of the figure. The curve displays the result of the DIAL equation, that is included at the bottom of the figure. The curve has an initial value of 1.0; decreases upon its passage through the first cloud, continues horizontally between the clouds, finally to sharply decrease on its passage through the final, dense cloud. At this point we note, that our initial pedagogical assumption of a uniform particle distribution was really not needed; localized particle clouds, e.g. those related to the gas emissions, would show up in the same way in the on- and off-resonance curves, and would thus disappear in the division leading to the DIAL equation. In this equation $P(\lambda_{on,off},R)$ is the backscattered intensity from a distance R for the laser wavelength $\lambda_{on,off}$ at which the gas has the absorption cross section $\sigma(\lambda_{on,off})$. N(R) is the density of absorbing gas molecules at a distance R. In

part d) the gas concentration curve N(R), obtainable through inversion of the DIAL equation, is shown. The simple form of the DIAL equation given in the figure can be derived using simplified, but frequently realistic assumptions, discussed in detail in Refs 1,2.

After this discussion of a typical mode of operation for the new system we will give a detailed description below, presenting the different subsystems of the new facility. A few measurement examples are then given to illustrate the system performance and the computer data representation routines. Finally, a number of further system applications are discussed.

2. System Description

2.1 Mobile Platform

The mobile laboratory is based on a Volvo F610 truck with a specially designed cargo compartment. An overview of the system is given in Fig. 3. The truck, which weighs almost 10 tons, carries three persons in the driver's cabin. The truck is equipped with four sturdy supporting legs that can be hydraulically lowered to achieve high stability during measurements requiring high directional accuracy in the optical system. The cargo compartment, constituting the optical laboratory, measures 6.0 x 2.3 x 2.1 m^3 (length x width x height). The walls are insulated and two windows and two skylights provide light and ventilation. An air-conditioner and a heater system are installed to control the laboratory milieu in a Nordic environment with an outside temperature varying from -20 ^{o}C in winter to +30 ^{o}C during the

summer.

The mobile laboratory houses two vibrationally isolated benches measuring 4.0 x 0.7 and 1.3 x 0.6 m^2. The longer one is intended for the laser equipment, while the other one can be used for different types of detection equipment. Two electronic racks and the frame for the vertically mounted telescope are also vibrationally damped. The rest of the equipment is securely mounted on the walls and on the floor of the compartment. Two operators can work in the front main computer/electronics region. A collapsable table/chair arrangement is attached to the one free side wall. A further convenient work station is available at the smaller, rear vibrationally isolated bench which is not occupied in normal lidar work. Beneath the floor of the laboratory there are several storage compartments, accessible from the outside.

To provide electric power to the laboratory in the field a 20 kVA motor generator is employed. The diesel engine and generator are installed in a sound-proofed covered trailer. In the mobile laboratory the power is split up into three lines, each capable of providing 220 V, 25 A, AC. When at its home base, the mobile laboratory is docked to a laboratory building employing the vehicle rear door and a matched building door surrounded by a cushioned sealing frame. The system is then hooked up to the normal mains line.

2.2 Telescope and Dome Mechanical Arrangements

A vertically mounted telescope looking up into a retractable transmitting/receiving dome is used in the present system. A layout of these units is given in Fig. 4. Such a configuration with optical exit/entry at the top of the laboratory provides 360^{o} horizontal access and excellent close-range laser safety. Further, the vertical stacking of the units is very favourable in saving valuable laboratory space. However, the substantial total height (4.2 m) of the operating system requires that the dome be retractable into the laboratory interior. This also provides additional protection during transport of the otherwise weather-proof dome and also yields service advantages. In Fig. 4 the dome is shown in a retracted position.

For the dome and telescope installation a self-supporting frame was built extending from the side walls across the roof of the vehicle. Two U-frames were used, one in front of and the other one behind the telescope to reinforce the laboratory construction.

The telescope and the dome carriage are guided sideways by ball bushings sliding along four rods attached to the framework and extending from floor to ceiling. These rods do not carry any weight but are instrumental in defining the position of the optical components. The telescope frame is supported from below by vibration isolators/shock absorbers. The primary telescope mirror is mounted at the rear of the telescope tube on an adjustable plate. The folding mirror deflecting the collected light into the detection unit is mounted on a fixed tripod in the telescope tube. The primary detection unit is bolted to the telescope frame to make it an integrated part of the telescope which is carefully enclosed to protect the optical

components from damage and dust.

The dome construction is fixed to the inner ring of 40-cm diam. ball bearing. The outer ring of this bearing is mounted in the dome carriage, which is guided by ball bushings sliding on the four rods. A stepping motor acting on a worm gear is used to turn the dome horizontally. One step from the stepping motor results in a 0.06 mrad change in direction. The dome consists of a stiff framework that carries the mirror mount on plain bearings. It also holds the vertical positioning mechanisms including a worm gear driven by a stepping motor. Each step tilts the mirror 0.08 mrad. A defroster fan is provided for the dome inside its weather-proof cover. After the dome is raised through the skylight, using a hand-driven winch, an additional rain cover is moved forward electrically, for protection against weather and stray light.

2.3 Optical Systems

In the current configuration, the laser transmitter is a Quanta-Ray DCR-1A Nd:YAG laser pumping a PDL-1 dye laser. The dye laser is equipped with two separate dye pump systems so that changes between blue and red dyes can be conveniently made. The pump laser is cooled by a 3 kW closed-loop cooling system. Other laser systems can also be used in the laboratory, e.g. other YAG systems, excimer or CO_2 lasers.

The dye laser wavelength is controlled by changing the grating angle. When a measurement is performed a fast-tuning device is used. An arm that is directly coupled to the grating is rapidly tilted by an excentric wheel driven by a stepping motor. The wheel revolves at

5 Hz, allowing two laser pulses per cycle if the pulse repetition frequency is 10 Hz. In this way "on" and "off" wavelengths can be generated corresponding to positions on the wheel separated by 180°. The phase setting of the wheel with respect to the laser firing determines the $\Delta\lambda$ value between zero and a maximum value. The $\Delta\lambda$ interval can be arbitrarily placed in the wavelength range covered by the dye used. This device gives a small wavelength jitter but this is no problem when species such as NO_2, SO_2 or O_3, all with relatively broad spectral features, are monitored. When very precise wavelength control is needed, as is the case with species such as NO and atomic mercury, a piezo scanning device is utilized[14]. Here a piezo crystal is coupled to the arm. It is controlled by the computer through a high-voltage supply. This gives more accurate wavelength control since the position of the piezo is very well defined. Normally it is driven at 5 Hz, providing "on" and "off" pulses.

Two different schemes are employed for calibration of the dye laser wavelength - absorption cell calibration or optogalvanic calibration. In the absorption mode a fraction of the dye laser beam intensity is split-off and divided into two beams by a 50% beam-splitter. One of the beams passes a quartz cell with the absorbing gas and the other beam is left unperturbed. Two photo- diodes record the beam intensities. When the dye laser wavelength is scanned, an absorption spectrum is recorded from which the dye laser can be calibrated. This mode can be used, for example, for NO_2 where a blue beam is used. In the optogalvanic method, the beam split off for calibration is directed to the cathode of a hollow-cathode lamp. The optogalvanic effect can be observed on an oscilloscope when the dye laser wavelength coincides with a line of the spectrum of the filling gas or of the cathode material. By recording the effect for a number of known

lines together with the dye laser setting a calibration can be made by applying a linear regression fit to the data. The absorption cells, the photo-diodes and the hollow-cathode lamp are all placed in a special calibration unit. The absorption measurements and the linear regression fitting are fully computerized.

The dye laser beam can be frequency-doubled with KD^*P crystals, Raman-shifted with a Raman-shifting cell or mixed with the fundamental Nd:YAG wavelength to produce sum- or difference- frequencies. All these devices can be incorporated into the optical system. The dye laser beam is directed into the telescope by a right-angle quartz prism. Another right-angle prism, mounted at the center of the tripod in the telescope, transmits the beam into the atmosphere. This prism controls the direction of the laser beam, which is normally coaxial with the telescope axis. Servo motors and micrometer screws offer remote control of the prism, through which the overlap between the laser transmission lobe and the telescope field of view is controlled. A tube shelters the beam in the telescope and minimizes the effect of stray light. A mechanical chopper, built into the tripod, can block the beam if desired. The computer-controlled chopper is automatically used during a lidar measurement in order to obtain the signal due to the background light only. Before the beam is sent out from the telescope it passes a 6x beam expander. This is done both to improve the beam quality and to protect the output mirror coating - the peak power density of a high-power pulsed laser is, in some cases, sufficient to burn a mirror coating, especially if ultraviolet radiation is employed.

A large flat mirror placed in the dome is used both for transmission and optical reception. It directs the laser beam and collects backscattered light and directs it down into the telescope. The dimensions of the mirror are 400 mm x 700 mm x 60 mm with a triangular segment with short sides 100 mm and 150 mm cut off at each corner. It is 60 mm thick in order to avoid any distortion of the beam. To protect the dome and to allow operation of the system during cold or rainy weather, a 450 mm x 600 mm quartz window seals off the dome. A Newtonian telescope with a focal length of 1 m receives backscattered light through the dome and the free opening is 400 mm. The folding mirror, mounted on a tripod, is flat and is elliptical with axes of 120 mm and 170 mm. Spherical aberration creates a minimum telescope field of view of 2 mrad, to be compared with the laser beam divergence of about 1 mrad. All mirrors are coated with aluminum and SiO_2, a standard coating that exhibits reasonably high reflectance throughout the spectrum. It is considerably more resistant than an MgF_2 coating, an alternative that was discarded since it is easily scratched and therefore not suitable for the very rough environment associated with field campaigns with a lidar/DIAL system.

The light enters the detection unit from the folding mirror. An adjustable field stop is placed in the focus, by means of which the field of view of the telescope can be varied from 2 to 5 mrad. After the focus the light is made parallel by a small quartz lens and the appropriate wavelength region is selected with an interference filter. Up to four filters can be placed in a wheel in the detection unit, thus making rapid changes of wavelength region possible. The laboratory is equipped with filters ranging from 227 nm to 2.3 microns to enable the detection of a large number of species. A detector (normally a PMT) is used to transform the optical signal into an

electrical one. An EMI 9558 QB or an EMI 9816 QA PMT is commonly used. The latter unit is the principal detector for our DIAL work. It has an S20 cathode, a high gain (10^7) and a fast risetime (2 ns). In order to compress the dynamic range of the signal to prevent detector overload the PMT is gain-modulated. The gain is very low when signals from close ranges are detected and then rises to the maximum value after 2-10 microseconds (the risetime is variable). The modulation circuitry resembles the one described by Allen and Evans[15] A TV system has been installed to facilitate setting and checking the direction of the laser beam. In the focal plane of the telescope, just in front of the adjustable field stop, a mirror directs the light into a TV camera. The mirror has a hole where the light passes onto the aperture and thus the TV picture will show the direction of the lidar. The position of the TV camera is adjusted with a stepping motor connected to a worm gear that rotates it so that the picture horizon is always horizontal irrespective of dome horizontal orientation. The stepping motor is driven by an angular caption device coupled to the horizontal dome rotation.

2.4 Electronics and Computer System

A schematic diagram of the system electronics is shown in Fig. 5. The signal from the light detector is preamplified and captured with a 100 MHz transient digitizer (LeCroy), that is capable of converting two independent analogue signals with 8-bit resolution into a 32 kb multichannel memory. (LeCroy units 6102, 2 x TR8818, 2 x NN 8103A, 8013). Normally 2048 channels, each 10 ns wide, are recorded, corresponding to a lidar measuring range of 3 km. After the recording, the data are transferred via a GPIB interface to the main computer

where they are added into a 32-bit data array. The computer is capable of transferring and adding two independent lidar signals at a 10 Hz repetition rate. The digitized signal is displayed on a 100 MHz oscilloscope (Leader Model LEO 518) through an output on the transient digitizer. The main computer (ITT XP) is an IBM-compatible personal computer with a floating point processor and 512 kb of primary memory. For the large amount of data involved in a lidar measurement a 20 Mb hard disk is used. After the measurement, the raw data are stored on a floppy disk as a backup. A graphical terminal with 720 x 350 pixels is used for operator interaction and data representation through a software package. Hard copies of data in various representations are obtained through a printer and a plotter.

2.5 System Steering

A plug-in card with a Z 80 CPU and some I/O lines performs the necessary real-time system steering. Upon request from the main computer the dome stepping motors, the dye laser wavelength wheel, the light chopper, the laser trigger etc. are activated. During a DIAL measurement the plug-in card takes care of the wavelength setting and the synchronization between the wavelength wheel, the laser trigger pulses and the light chopper, while the main computer is transferring and adding lidar curves. Besides system steering through the computer, it is possible to direct the dome using manual switches both at the telescope and the operator position. Many other controls and switches (main power, dome cover, dome defroster, PMT high voltage etc.) are also conveniently placed in the main rack. A display showing the horizontal and vertical angular positions of the dome is placed in front of the operator. These values are automatically compared with manually set upper and lower limits to prevent accidental dome

movements outside shooting boundaries. Should a boundary be passed the dome movement stops and blinking LED's alert the operator. This procedure provides additional eye safety when operating in urban areas.

2.6 Software Description

For a description of the organization of the system software we refer the reader to Fig. 6. The computer software, which is written in Pascal, consists of several library procedures for system steering, data transfer, disk I/O operations and graphical presentation. Such library procedures are then combined into several menu-oriented main procedures, each with a specific task. In preparation for a DIAL measurement several horizontal or vertical scans can be defined with a specific starting point and given angular separations between the directions in the scan. Three different scans with up to 15 directions each can be defined. The phase angles of the excentric wheel at laser firings and the total number of measurement cycles in each direction are also given. A DIAL measurement cycle consists of 8 shots on each wavelength, fired alternately, and finally two shots with the chopper closed. Several cycles are then averaged and stored on the hard disk after background subtraction, before the next direction is set. After completion of the measurement the operator is asked if a backup of the recorded data is required. Otherwise the data are erased when the next measurement takes place.

In the DIAL evaluation part of the software, it is possible to visualize all stages in the evaluation. This makes it easier to optimize the parameter settings. Both linear and Gaussian smoothing functions can be used on the raw on- and off-wavelength curves and also on the ratio curve. The width of the smoothing function can be chosen. A running average function of adjustable width is used to evaluate the concentration as a function of distance. Routines for evaluation of particle measurements (normal lidar measurements) are included separately. When the parameter settings are satisfactory a concentration map is automatically made from the measurements, presented on the graphic screen and hard-copied if requested. This program feature turns the normally complicated DIAL evaluation and result representation work into an easy routine and the result of the measurements is almost immediately available in a compact and user-oriented form.

3. Examples of Measurements

Some field measurements have been performed with the mobile lidar system during a one-year period and a few examples will be given here to illustrate the system performance and the different data representation forms available.

Fig. 7 shows an example from a DIAL measurement on a plume containing SO_2 where the data are displayed according to Fig. 2. The curves in Fig. 7a show the detected signal intensity due to backscattered laser light for the on- and off-resonance wavelengths, which in this case are 300.03 nm and 299.33 nm, respectively. The curves display the sum of 50 cycles corresponding to 400 shots at each wavelength with the

background light level subtracted. The gain modulation is set to reach the maximum value at a distance of about 600 m and this value is retained until 40 μs after the laser firing, corresponding to a distance of 6 km. As can be seen from Fig. 7a, the plume located between 900 and 1000 m from the lidar system site also contains aerosols, evidenced by the increased backscattering and a part of the attenuation through the plume. The aerosol dependence is eliminated by taking the ratio of the on and off signal, which is shown in Fig. 7b, where the slope in the plume is determined by the difference in absorption cross section for the two wavelengths. Thus, by using known values for the SO_2 cross section[16] the concentration N(R) can be evaluated by inverting the equation shown in the lower part of Fig. 2. Fig. 7c shows the concentration profile along the laser beam, evaluated for a 70-m interval continuously swept with the distance, i.e. the value at distance R is the mean concentration for the path R +/- 35 m. The resulting noise can also be inferred from Fig. 7c, showing the increased noise level at greater distances due to the $1/R^2$ fall-off and plume attenuation of the signal. If range resolution is not so critical, a lower noise level and thus a lower detectable concentration can be achieved if a longer evaluation interval is employed. For ranges up to 1 km the detection limit of the integrated concentration is typically 5 $mg/m^3 \times m$ [10].

It is often interesting to chart the gas concentration in a horizontal or vertical section. This can be achieved by performing several sequential measurements such as the one displayed in Fig. 7, for different directions. Fig. 8 shows an example of such a measurement, where the SO_2 concentration is mapped in a vertical section downwind from a paper mill. Fifteen different vertical directions were used, each consisting of 50 measurement cycles. Thus

the time for the complete scan was about 20 min. The map with an 8-level grey scale can be presented by the computer only a few minutes after the measurements. If a more representative charting over a longer time period is required or in order to get better statistics, several scans can be averaged and a mean picture presented. The possibility of making concentration maps is a unique and very useful application of the DIAL technique. A vertical scan like the one displayed in Fig. 8 can also be used to measure the flux of SO_2 passing through the vertical section. The concentrations are then integrated over the area of the plume cross section, and the integrated content is multiplied by the wind velocity normal to the vertical section. In this way, diffuse emissions from a plant can also be captured and the total flow of a particular gas from the industry be measured. In the example given in Fig. 8 the total flow was found to be 230 kg/h of SO_2.

Fig. 9 shows an example of another way of presenting data from a vertical scan. Besides the charting, a horizontal projection of the plume is displayed. Here the distribution of both the SO_2 plume and the partly overlapping particle plume are shown. The particle concentration is given in relative units and is evaluated from the off-resonance wavelength in the SO_2 DIAL measurement. The measurement curves have been divided by the curve resulting from a measurement in a particle-free direction - normally one of the upper directions in the sweep. This compensates for system factors, gain modulation, $1/R^2$ dependence, and clean-air attenuation. When dense particle plumes are monitored, the beam will suffer severe attenuation when it propagates through the cloud, and this should also be corrected for. In this case, however, the correction was not needed. A horizontal projection is, in many cases, a more useful presentation mode and can, for

instance, be copied directly onto a map of the industrial area to localize different sources. Vertical and horizontal projections are also well suited in studies of plume dispersion.

NO_2 is another pollutant of great interest, especially in urban areas. NO_2 can be measured with DIAL techniques in the blue spectral region near 450 nm. The high intensity of background light in the atmosphere at these wavelengths makes the use of a narrow-bandwidth interference filter necessary. The gain modulation of the detector is also crucial to make measurements during daytime possible, keeping the mean power dissipation in the PMT at an acceptable value. Fig. 10 shows an example from an NO_2 measurement in a ground inversion situation[17]. This is a situation where the air close to the ground is trapped by a warmer layer of air, leading to the build-up of a high pollutant concentration. During the measurement the creation, build up and breakdown of the inversion was studied by monitoring the NO_2 concentration over a large area at different times during the day. Fig. 10 shows an NO_2 concentration map obtained by scanning the laser horizontally. A vertical scan for one of the directions is also inserted. The total measurement time required to obtain the map presented here was one hour. A measurement like this one can also be useful in determining the most interesting paths for long-path absorption instruments like a DOAS instrument[3,4]. The DOAS technique is then used to routinely monitor the mean concentration over one or several paths which the DIAL measurement has shown to be of interest.

4. Discussion

The measurement examples discussed above illustrate the power of the system in performing DIAL measurements. The new evaluation and representation routines eliminate hours of manual evaluation effort and transform an exclusive research system into a realistic method for practical near-real-time pollution assessment. Apart from SO_2, NO_2, and O_3 monitoring, readily performed with the system as it is described above, many other gases can be studied with modified equipment. Since ample space for laser transmitter and detection equipment is provided, various other lasers apart from a Nd:YAG-based system, can be employed, and even quite large spectrometer systems can be utilized for the signal analysis. A high spectral resolution on the detection side is of particular importance in many DOAS applications. Techniques for the monitoring of previously little- studied constitutents can be investigated at a level of increased hardware complexity. Besides pollution studies, atmospheric gas anomalies might be used for ore and geothermal energy exploration, e.g. using atomic mercury as a tracer gas[18-20]. For remote studies of laser-induced fluorescence a powerful UV source could be combined with array detector techniques. In this way possible environmental fluorescence anomalies, e.g. due to vegetational stress, may be investigated[21]. We also foresee that the present system can have important applications as regards bringing out advanced electro-optical and computer equipment into industrial milieuxs while at the same time being in the locally protected and dustfree environment provided by the mobile laboratory. In such applications open laser beams may be employed but fiber-optical transmission lines, utilizing advanced spectroscopic sensor techniques will probably be used more frequently. In this way new techniques for technical combustion studies[13], surface

monitoring[22], chemical process steering etc. may be developed.

Acknowledgements

This work was supported by the Swedish National Environment Protection Board (SNV) and the Swedish Space Corporation (SSC). Support and encouragement from Göran Persson, SNV, and Claes-Göran Borg, SSC, are gratefully acknowledged. The skilful work of J. Bergin, Å. Bergquist, B. Hermansson, R. Olofsson and G. Werner of the Physics Department workshops and the assistance of K. Stridh in the design work was critical to the successful completion of the project. The contributions by Bo Galle, The Swedish Environmental Research Institute, to the software development are much appreciated.

References

1. D.K. Killinger and A. Mooradian, Eds. Optical and Laser Remote Sensing, Springer Series in Optical Sciences, Vol. 39 (Springer, Heidelberg, 1983).

2. R.M. Measures, Laser Remote Sensing (Wiley Interscience, New York 1984).

3. U. Platt and D. Perner, in Ref. 1.

4. H. Edner, A. Sunesson, S. Svanberg, L. Uneus and S. Wallin, Appl. Opt. 25, 403 (1986).

5. K. Fredriksson, B. Galle, K. Nyström and S. Svanberg, Appl. Opt. 18, 2998 (1979).

6. K . Fredriksson, B. Galle, K. Nyström and S. Svanberg, Appl. Opt. 20, 4181 (1981).

7. K. Fredriksson and S. Svanberg, in Ref. 1.

8. A.-L. Egebäck, K.A. Fredriksson, and H.M. Hertz, Appl. Opt. 23, 722 (1984).

9. K.A. Fredriksson and H.M. Hertz, Appl. Opt. 23, 1403 (1984).

10. K. Fredriksson, Report SNV PM 1639 (1982).

11. H. Edner, S. Svanberg, L. Uneus, and W. Wendt, Opt. Lett. 9, 493 (1984).

12. P.S. Andersson, S. Montán and S. Svanberg, to appear.

13. M. Aldén and S. Wallin, Appl. Opt. 24, 3434 (1985).

14. J. Kamme, Diploma Paper, Lund Reports on Atomic Physics LRAP - 65 (1986).

15. R.J. Allen and W.E. Evans, Rev. Sci. Instr. 43, 1422 (1972).

16. D.J. Brassington, Appl. Opt. 20, 3774 (1981).

17. B. Galle, A. Sunesson, and W. Wendt, Submitted to Atmospheric Environment

18. Q. Bristow and I.R. Jonasson, Can. Min. J. 93, 39 (1972).

19. V.Z. Fursov, N.B. Voltson, and I. Khvalovskly, Dokl. Akad. Nauk SSSR 179, 208 (1968).

20. J.C. Varekamp and P.R. Buseck, Geothermics 12, 29 (1983).

21. F.E. Hoge and R.N. Swift, Appl. Opt. 20, 3197 (1981).

22. S. Montán and S. Svanberg, Appl. Phys. B 38, 241 (1985).

Figure Captions

Fig. 1 Photograph of the mobile remote sensing laboratory with its motor generator trailer.

Fig. 2 Illustration of the principle of differential absorption lidar (DIAL).

Fig. 3 Schematic view of the mobile remote sensing system.

Fig. 4 The telescope and optical dome arrangements.

Fig. 5 Overview of the system electronics.

Fig. 6 Organization of the computer software.

Fig.7 Illustration of a DIAL measurement of SO_2. a) On- and off-resonanace lidar curves obtained by averaging 400 3 mJ laser shots for each wavelength. b) Ratio (DIAL) curve showing the presence of SO_2. c) SO_2 concentration curve evaluated from b).

Fig. 8 Mapping of a cross section of an SO_2 plume from a paper mill obtained by DIAL measurements for 20 minutes.

Fig. 9 Simultaneous mapping of SO_2 and particles. The particle density is given in relative units (R.U.).

Fig.10 Mapping of NO_2 during an inversion episode. Data displayed are recorded for a total measuring time of one hour using 5 mJ laser pulses at a repetition frequency of 10 Hz.

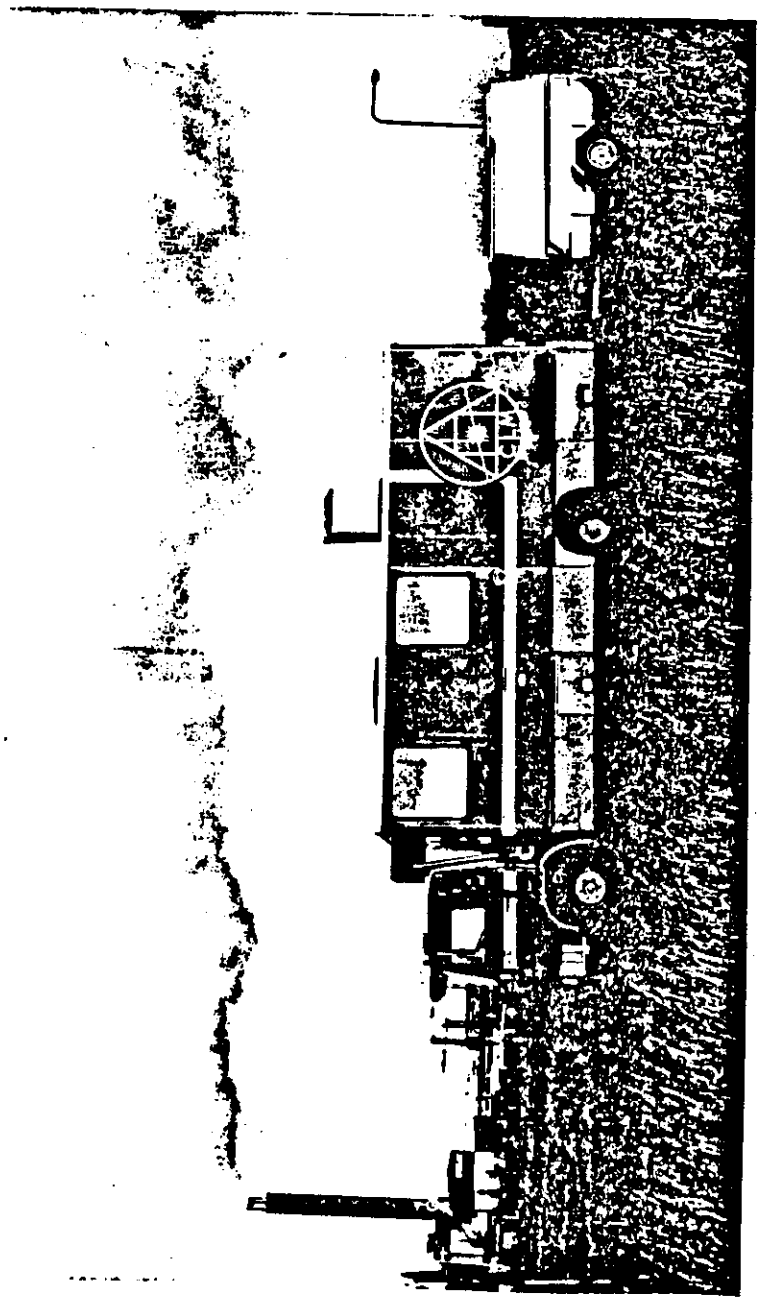

Figure 1

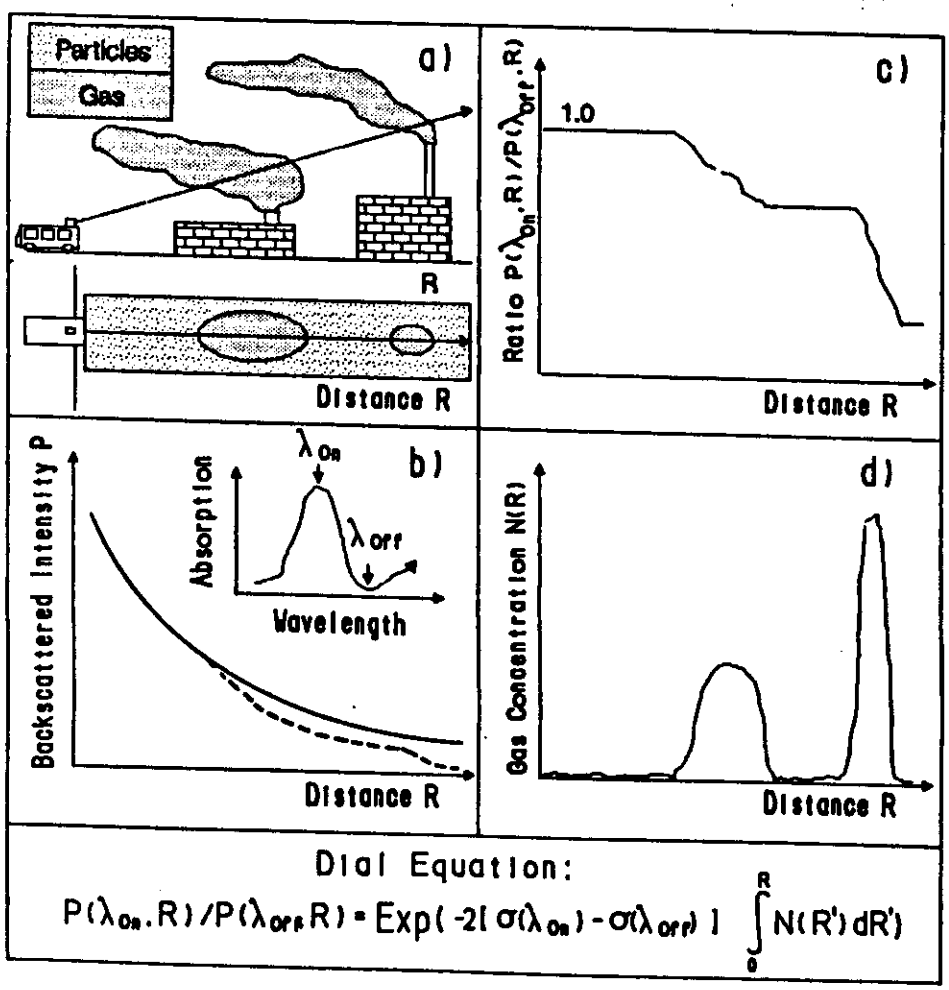

Figure 2

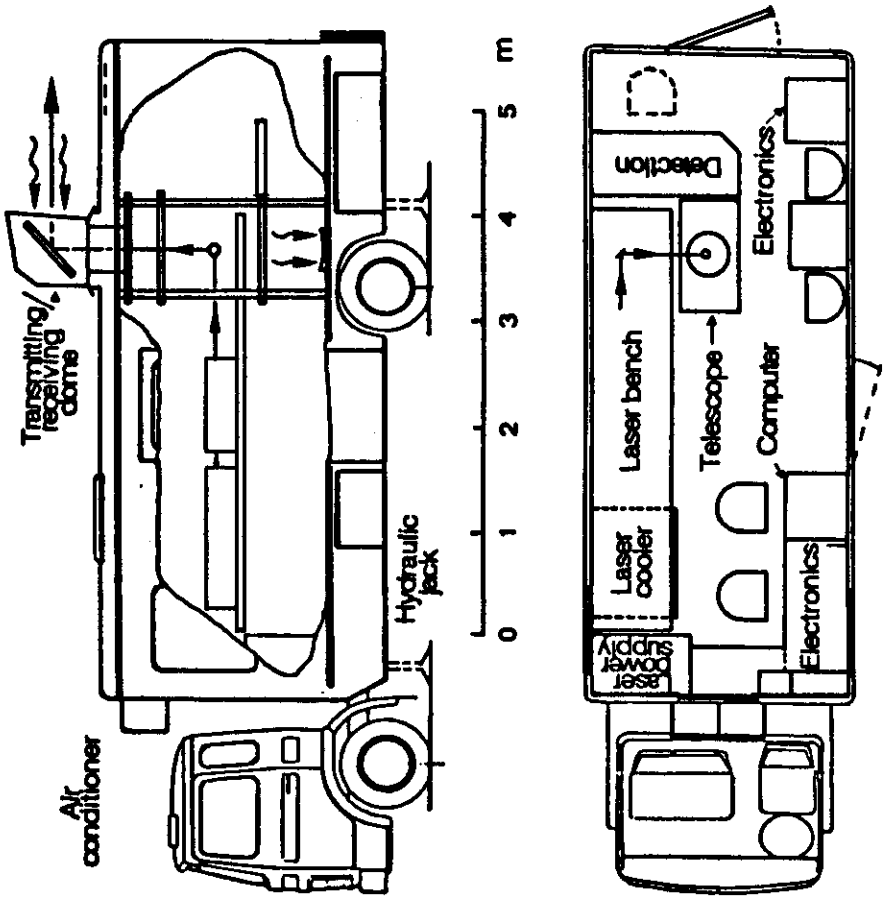

Figure 3

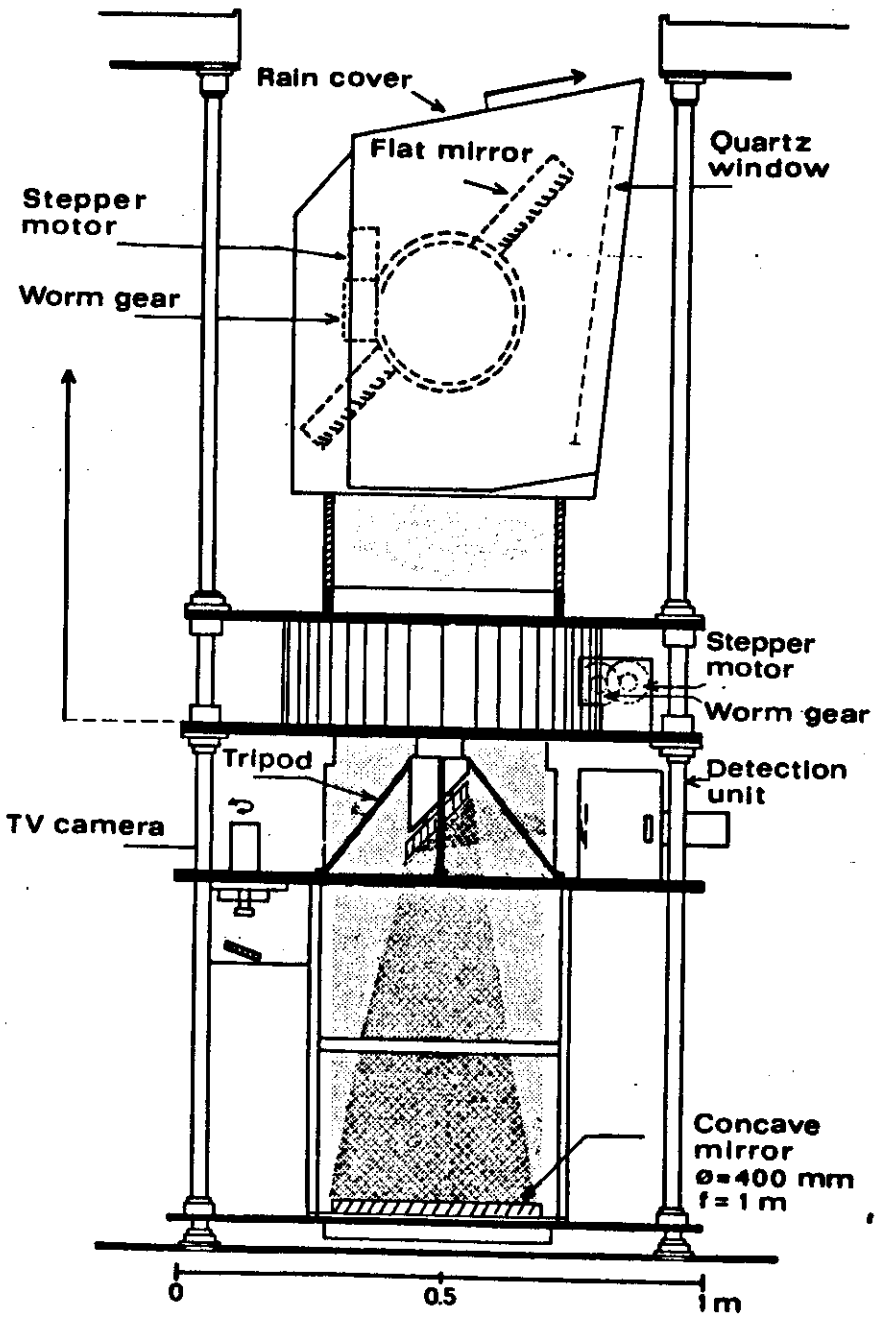
Rain cover
Flat mirror
Quartz window
Stepper motor
Worm gear
Stepper motor
Worm gear
Tripod
Detection unit
TV camera
Concave mirror
ø=400 mm
f=1 m
0
0.5
1m

Figure 4

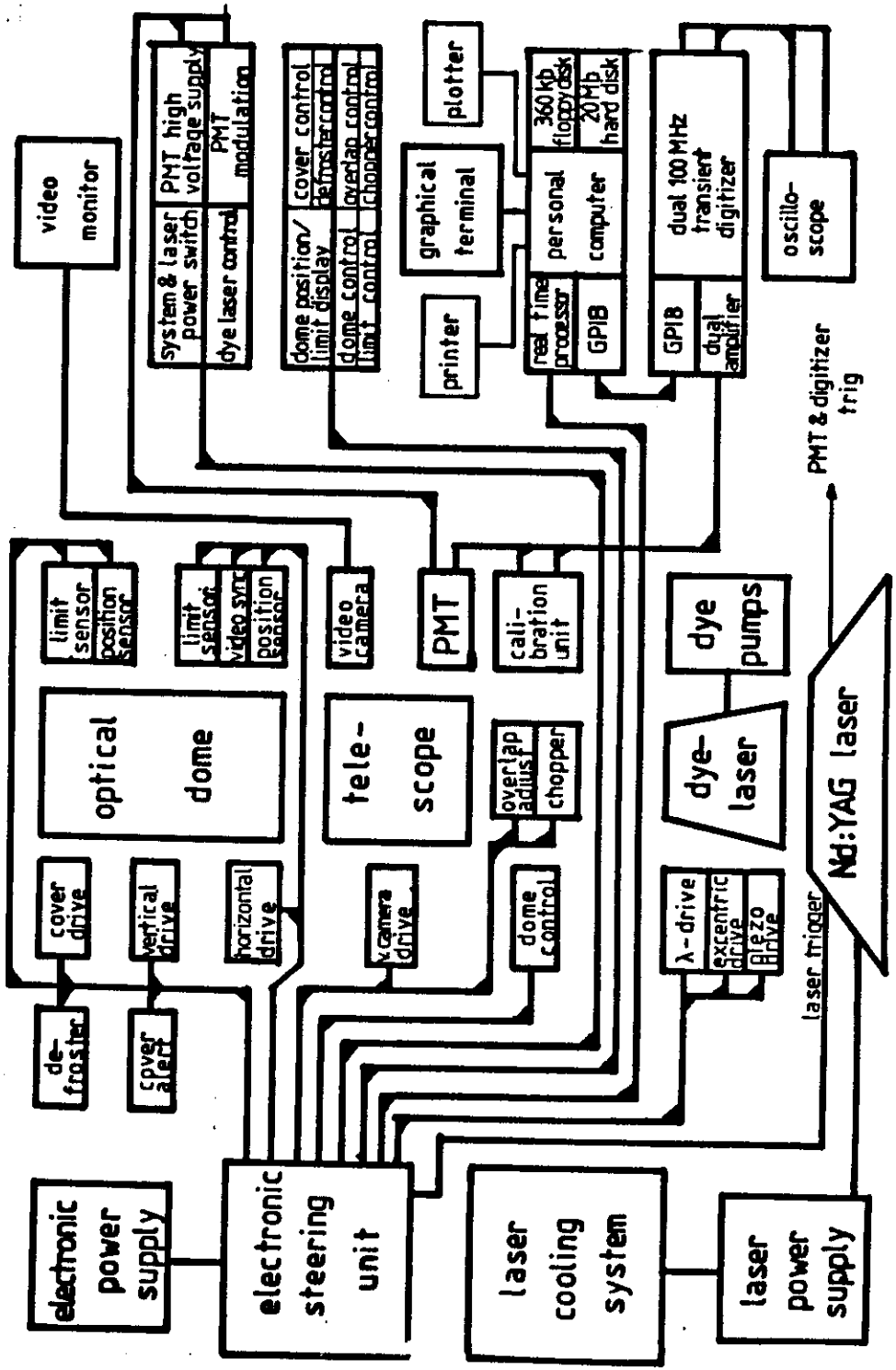
video monitor
PMT high voltage supply
PMT modulation
system & laser power switch
dye laser control
dome position/ limit display
cover control
defrostercontrol
dome control
overlap control
limit control
chopper control
plotter
graphical terminal
printer
360 kb floppy disk
20Mb hard disk
personal computer
real time processor
GPIB
dual 100 MHz transient digitizer
GPIB
dual amplifier
oscillo-scope
PMT & digitizer trig
limit sensor
position sensor
limit sensor
video sync
position sensor
video camera
PMT
cali-bration unit
dye pumps
optical dome
tele-scope
overlap adjust
chopper
dye-laser
Nd:YAG laser
cover drive
vertical drive
horizontal drive
x camera drive
dome control
λ-drive
excentric drive
piezo drive
laser trigger
de-froster
cover alert
electronic power supply
electronic steering unit
laser cooling system
laser power supply

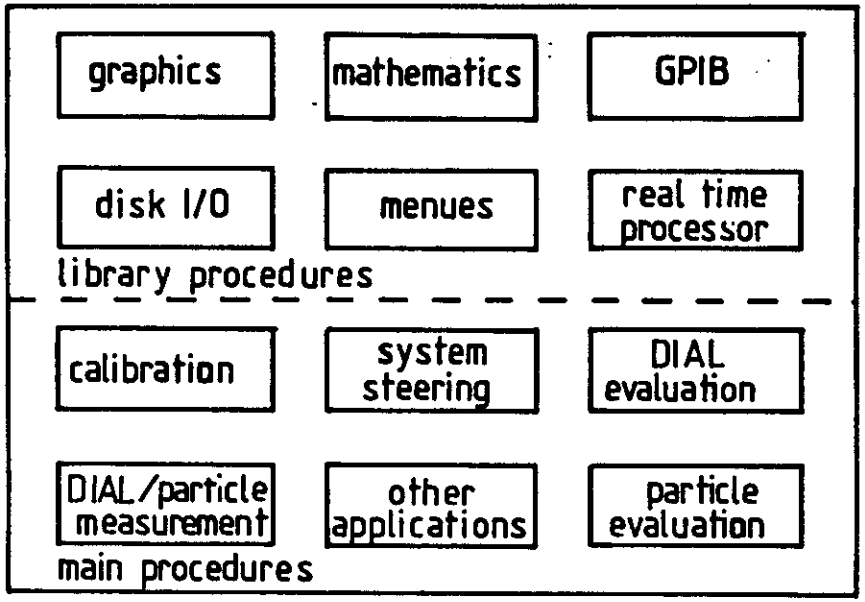
graphics
mathematics
GPIB
disk I/O
menues
real time processor
library procedures
calibration
system steering
DIAL evaluation
DIAL/particle measurement
other applications
particle evaluation
main procedures

Figure 6

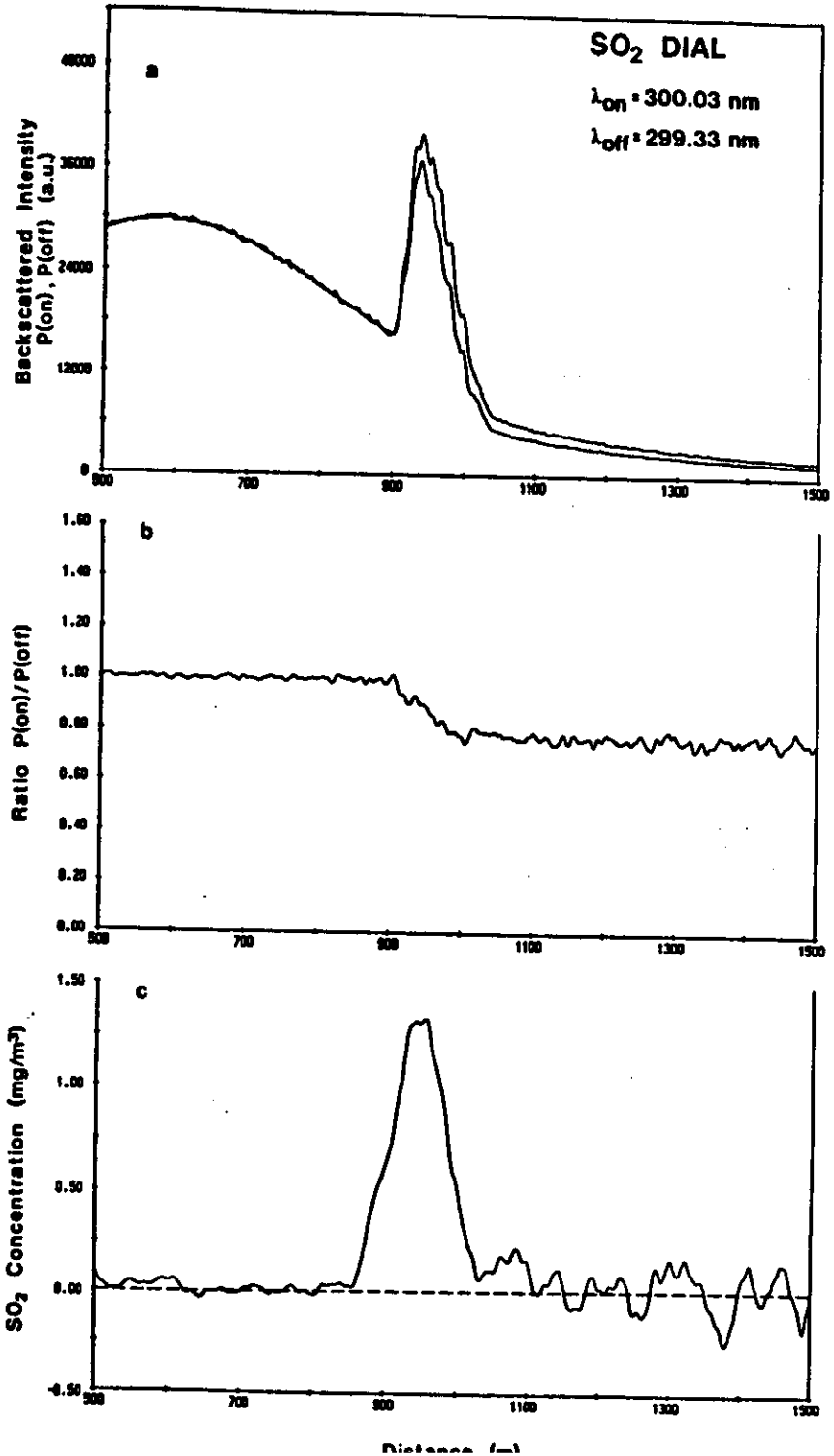
SO2 DIAL
λon = 300.03 nm
λoff = 299.33 nm
a
Backscattered Intensity P(on), P(off) (a.u.)
b
Ratio P(on)/P(off)
c
SO2 Concentration (mg/m³)

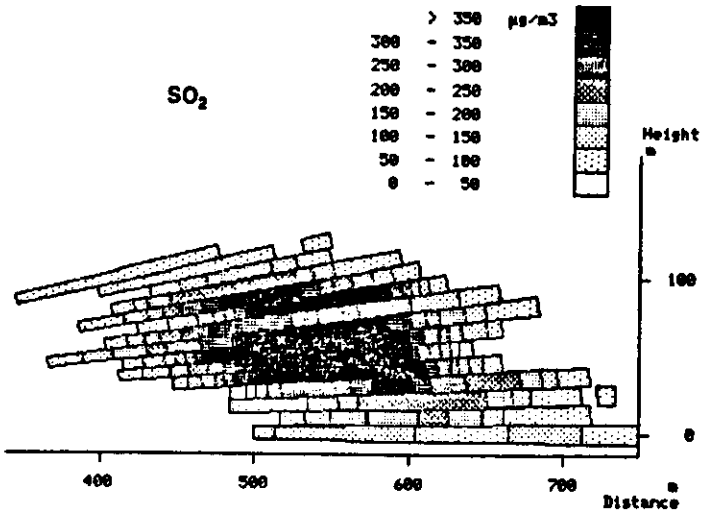

Figure 8

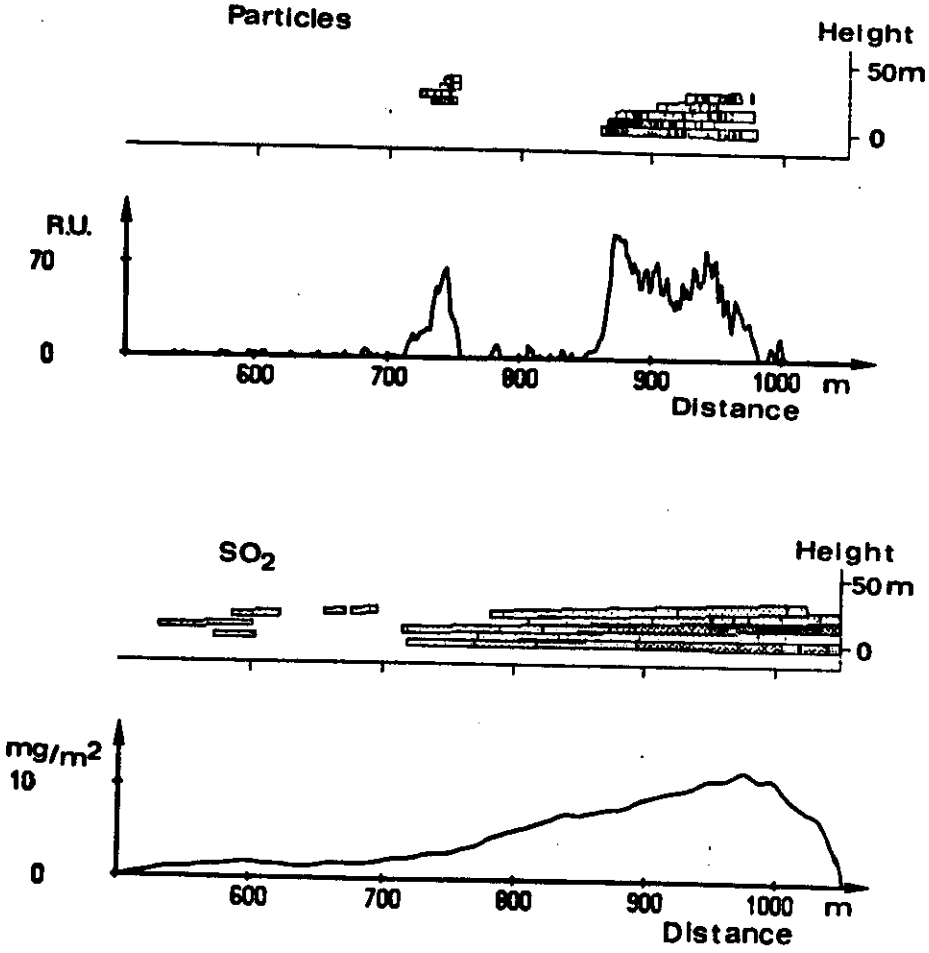

Figure 9

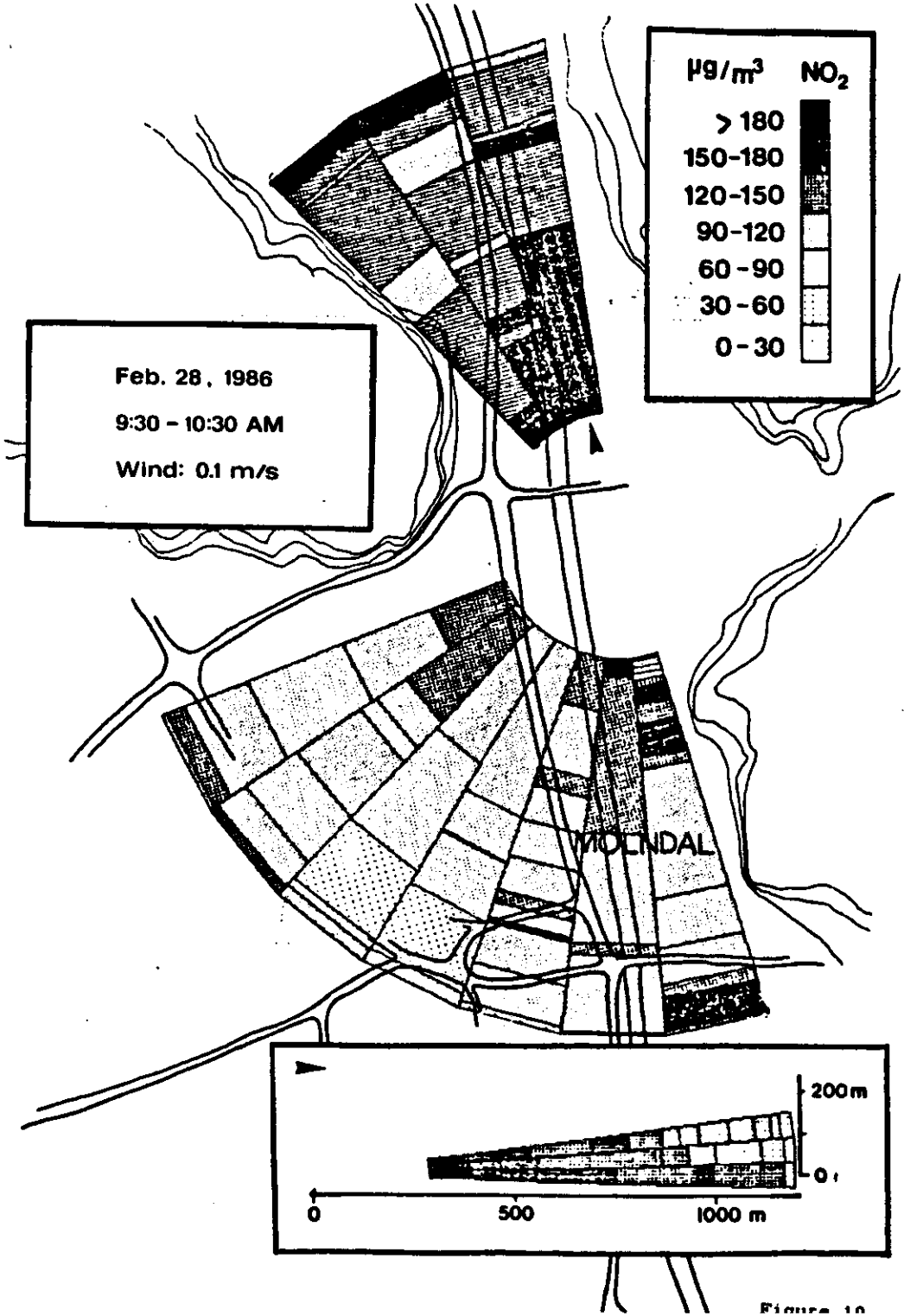
µg/m³ NO₂
> 180
150-180
120-150
90-120
60-90
30-60
0-30
Feb. 28, 1986
9:30 - 10:30 AM
Wind: 0.1 m/s
MOLNDAL
200m
0
0
500
1000 m

Figure 10